Article

SERS chemical enhancement by copper - nanostructures: Theoretical study of Thiram pesticide adsorbed on Cu$_{20}$ cluster

Truong Dinh Hieu[1,2], Ngo Thi Chinh[1,2], Nguyen Thi Ai Nhung[3], Duong Tuan Quang[4], Dao Duy Quang[1,5*]

[1]*Institute of Research and Development, Duy Tan University, Da Nang, 50000, Viet Nam*

[2]*Faculty of Natural Sciences, Duy Tan University, Da Nang, 50000, Viet Nam*

[3]*Department of Chemistry, University of Sciences, Hue University, Hue City, Thua Thien Hue 49000, Viet Nam*

[4]*University of Education, Hue University, Hue City, Thua Thien Hue 49000, Viet Nam*

[5]*Department of Environmental and Chemical Engineering, Duy Tan University, Da Nang, 50000, Viet Nam*

Abstract

Surface-enhanced Raman spectroscopy (SERS), a surface-sensitive technique, allows the practicability of detecting chemical compounds in ultra-low concentration. In this work, a chemical enhancement mechanism of SER process of Thiram pesticide adsorbed on copper nanomaterial surface was proposed based on density functional theory (DFT) approaches. Structural and electronic properties of Thiram and Thiram-Cu$_{20}$ complexes were optimized using PBE method with LanL2DZ basis set for copper atoms and cc-pVDZ basis set for the non-metal atoms. In the most stable adsorption configuration, Thiram interacted with Cu$_{20}$ cluster *via* two S(*sp^2*) atoms. The main peaks on normal Raman spectrum of Thiram were characterized at 371, 576, 1414 and 1456 cm^{-1} responsible for the stretching vibrations of C–S, C=S, S–C–S and C–N groups, respectively. Otherwise, the main peaks of Thiram-Cu$_{20}$ SERS spectrum were found at 534, 874, 982, 1398 and 1526 cm^{-1} corresponding to the stretching vibrations of S–S, C-S, S–C–S, C–N and CH$_3$–N bonds, respectively. The SERS chemical enhancement of Thiram by Cu$_{20}$ cluster was about 2 and 6 times stronger than those obtained from Ag$_{20}$ and Au$_{20}$ cluster, respectively. The chemical enhancement mechanism was also explained by analyzing HOMO and LUMO energies gap and density of states.

Keywords. Thiram, copper cluster, Raman, SERS, DFT.

1. INTRODUCTION

Pesticides are chemical compounds used in modern agriculture to kill insects, fungus, bacteria, weed and rodents. They are respectively named as insecticides, fungicides, bactericides, herbicides and rodenticides. By the structure, pesticides can be divided into organochlorines, organophosphates, carbamates and triazines.[1,2] An increasing utilization of pesticides in agriculture results in several severe problems on environment and human health.

Thiram (tetramethyl-thiuram disulfide or bis(dimethyl-thiocarbamoyl) disulfide) (C$_6$H$_{12}$N$_2$S$_4$) is a carbamate-categorized pesticide. Its molecular structure has two dimethyl-dithio-carbamate groups – (CH$_3$)$_2$N–CS$_2$ linked together by a disulfide bridge (S–S). Thiram has been used in many countries as fungicide to protect fruits, vegetables, ornamental and turf crops from a variety of fungal diseases.[3-6]

This compound is also used to protect fruit trees and ornamental fruits from damage of rabbit, rodent and deer.[7]

For many decades, surface-enhanced Raman spectroscopy (SERS) has intensively been investigated for its electromagnetic field enhancement near the nano-scale metallic surfaces of coinage metals (*i.e.* gold, silver and copper). Despite of intensive research attempts SERS chemical enhancement mechanism is still unclear mainly due to the relatively complicated enhancing factors and inconsistent experimental results. The advantages of SERS are that it magnifies Raman signals corresponding to the adsorbed compounds from 10^6 to 10^{10} times. Therefore, SERS technique has increasingly been utilized to improve detection of chemicals at trace concentrations. Attracted by its great advantages, many researches have employed SERS to analyze different chemical pesticides,

including Thiram, accumulated either in the environment or in agricultural products.

Kang *et al.* analyzed the SERS spectrum of Thiram adsorbed on silver surface.[8] Their results revealed that the peaks of Thiram located in the region below 1000 cm^{-1} (related to C–S, C–S–S assignments) are decreased or even disappeared in the SERS spectrum; whereas, others characterized for C–N and CH$_3$NC are enhanced, especially C–N stretching mode at 1372 cm^{-1}. These phenomena were also confirmed by Verma *et al.* using silver nanodendrites.[9]

The prediction of Raman and SERS spectra has commonly been investigated using density functional theory (DFT). Metallic cluster models are often used to reproduce nanoparticle surface. The complexes produced from interaction between an analyzed ligand and a metallic cluster can be utilized to predict their SERS spectra. Rajalakshmi *et al.* determined geometrical and electronic structures of 2-propylpiridine-4-carbothioamide as well as studied infrared, Raman spectra.[10] In their work, various DFT functionals including PBEPBE, SVWN, HCTH, B3LYP, mPW1PW91, B3PW91 combined with aug-cc-pVDZ basis set were chosen as computational strategies for spectra prediction. The research indicated that the B3LYP/aug-cc-pVDZ model results in the lowest deviations in the prediction of structure and vibrational spectra. Recently, An *et al.* investigated surface-enhanced Raman scattering of melamine (C$_3$H$_6$N$_6$) on silver substrate using experimental and DFT studies with the B3LYP/6-31G(d) method.[11] Silver cluster models including Ag$_4$, Ag$_8$, Ag$_{10}$ and Ag$_{20}$ were used to reproduce silver substrate. It was found that the small size clusters like Ag$_4$ can be an effective predictor for Raman and SERS spectra of melamine. This research also showed that the enhancement of typical peaks localized at 676 and 983 cm^{-1} were correctly predicted and consistent with the corresponding experimental results.
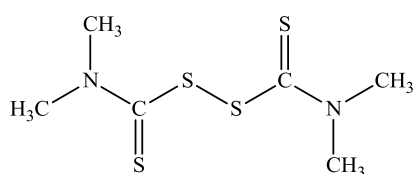
Figure 1: Molecular structure of Thiram

This study investigates Raman and SERS spectra of Thiram pesticide (figure 1) adsorbed on copper substrate using Cu$_{20}$ cluster model. The Raman spectrum of Thiram is projected and compared with the experimental data from the literature. SERS spectrum of Thiram adsorbed on Cu$_{20}$ cluster is predicted and compared with the spectra obtained by the corresponding investigations on Ag$_{20}$ and Au$_{20}$ clusters in order to demonstrate the effectiveness of copper substrate for SERS technique. Finally, a chemical enhancement mechanism is proposed providing more insight for SERS phenomenon. To the best of our knowledge, there have been an insignificant number of experimental and computational studies in the literature on SERS of chemical compounds adsorbed onto the surface of copper nanoparticles.

2. COMPUTATIONAL METHOD

All the DFT calculations were carried out using Gaussian 16, revision A.03.[12] The chosen DFT method was PBE[13] combined with the LanL2DZ basis set for metallic atom (*i.e.* Cu, Au, Ag) and the cc-pVDZ basis set for the non-metallic atoms. Different configurations of interactions between Thiram and Cu clusters were analyzed. The most stable Thiram-Cu$_{20}$ complex was used to project the corresponding SERS spectrum. It was then compared with the spectra obtained from Thiram-Au$_{20}$ and Thiram-Ag$_{20}$ complexes in an attempt to explain the influence of cluster nature on SERS enhancement. The scaling factor for harmonic frequencies of PBE/cc-pVDZ method was 1.0353.[14] Gaussum[15] was used to investigate density of states.

3. RESULTS AND DISCUSSION

3.1. Structure of Thiram

Figure 2 shows optimized structure, the highest occupied molecular orbital (HOMO), the lowest unoccupied molecular orbital (LUMO) distributions and electrostatic potential (ESP) map of Thiram in vacuum. The experimental structural parameters of Thiram are also included.

The structural parameters obtained from the PBE/cc-pVDZ level of theory are in good agreement with the experimental values. The difference between the respective bond lengths varies from 0.020 to 0.042 Å, within the deviation of 1.4-2.8 %. The calculated C11–S1–S2–C12 dihedral angle is 86.6^o which is in accordance with the measurement gained from experiments (*i.e.* 88.3^o). In the C$_2$NCS$_2$ group, all the atoms are nearly coplanar given the data ∠S3–C11–N5–C7 = 4.7^o, ∠S1–C11–N5–C8 = 3.5^o, ∠S1–S3–C7–C8 = 4.2^o. These imply a *sp^2* -hybridized structure of N and C atoms. In fact, C7–N5–C8 and C7–N5–C11 angles are equal to 118.6^o and 118.0^o, respectively, which are far from the characteristic angle of an *sp^3* hybridization (109.5^o);

also S3–C11–N5 (124.9°) and S1–C11–S3 (124.0°) angles are also close to 120°, the typical angle of an sp^2 hybridization. The bond angles at each S atom of S–S bridge (i.e. C12–S2–S1 and C11–S1–S2) are 102.5°. These values are smaller than sp^3 angle (109.47°). The reason of this is the influence of two free electron pairs in each S atom. These electron pairs occupy large space and make the C–S–S bond angle smaller. But this difference is not too big. Therefore, S1 and S2 are in sp^3 hybridization.
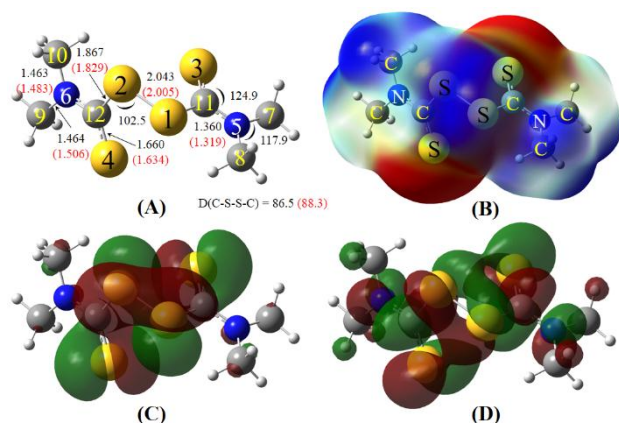
Figure 2: (**A**) Optimized structure, (**B**) ESP map, (**C**) HOMO and (**D**) LUMO of Thiram. Bond lengths are in Å, angles are in degree. Values in parentheses highlighted in red color are experimental values of Kang *et al.*[8]

The ESP map given by figure 2B illustrates the charge distribution of molecules in a three-dimensional simulation, which allows a determination on how the molecule interacts with exotic agents. In principle, the regions colorized in red represent the most negative atomic zones, prone to be attacked by electrophilic species; whilst, blue regions exhibit the most positive charges, conducive to an interaction with nucleophile species. This suggests that the S(sp^2) atoms possess the highest negative potential due to the +M effect of neighboring N and S(sp^3) atoms, while the most positive potential is observable localizing at S–S and CH$_3$ groups. The high significance of positive charge at these groups can be explained by the –M effect of the C=S bond and the electron deficiency on N atom. Therefore, S(sp^2) atoms are expected to donate electrons to an external electrophilic agent; whereas, S–S and CH$_3$ groups can are more likely to accept electrons from a nucleophilic counterpart.

HOMO and LUMO distributions in Thiram structure are shown in Figures 2C and 2D. HOMOs localize around the C–S–S–C group and two S(sp^2) atoms. Besides, N and C(sp^3) atoms are surrounded by smaller HOMOs. Therefore, the C–S–S–C group

and the S(sp^2) atoms of Thiram are predicted exhibiting high tendency to donate electrons. Otherwise, LUMOs are mainly distributed around S, N and C(sp^3) atoms. Thus, if a Thiram molecule is allowed to interact with a metal cluster, these regions are expected to accept electrons and form an interactive bond. The results are also highly consistent with those gained from ESP map.

If Thiram is adsorbed onto the surface of a copper crystal, electron transfer may occur. In detail, the regions in the adsorbent molecule localized by high negative potential or large HOMOs may interact with the copper cluster via donation of electrons to the clustering atoms. Reversely, the regions owing high positive charge or large LUMOs are predicted to accept electrons transferred from copper cluster. The stronger electronic exchange formed, the more stable the complexes. In particular, Thiram may interact with copper cluster *via* the position of atoms S, especially at the S(sp^2) atoms.

3.2. Structure of Thiram-Cu$_{20}$ complexes

Figure 3 shows structures and relative energies of seven complexes representing for all possible interactions between a Thiram molecule and Cu$_{20}$ cluster. Relative energy of each complex is calculated by the difference of the according enthalpy value with the lowest one.

Thiram molecule attends to interact with at a edge of pyramidal Cu$_{20}$ cluster *via* two or three sulfur atoms. The interacting modes **A** and **B** are obtained by the complexation between two S(sp^2) atoms (*i.e.* S3 and S4) with two copper atoms. In detail, the complex **A** comprises the interactions occurring at top of the cluster, and the interaction in complex **B** is observed at the center of one edge on the pyramidal cluster. Mode **A** is the most stable complex with the lowest relative energy (ΔE = 0.0 kcal/mol). This is followed by mode **B** with the value of ΔE 4.2 kcal/mol higher. Modes **C** (ΔE = 7.4 kcal/mol) and **D** (ΔE = 12.9 kcal/mol) correspond to the interactions at S2 and S3 atoms with two other respective copper atoms located at the top and at the edge of the copper clusters, respectively. Finally, the adsorption modes **E**, **F** and **G** are built through the interactions between 3 sulfur atoms (one S(sp^2) atom and two S(sp^3) atoms) with the copper cluster. The relative energies of these modes are significantly higher than the energy of mode **A**, varying within 9.6-12.6 kcal/mol. Thus, a Thiram-Cu$_{20}$ complex is predicted most stable if the S(sp^2) atoms in the Thiram molecule interact with cluster-copper atom at the top of the cluster.

In addition, the S(sp^2) atoms are more favorable to approach the cluster than their sp^3– hybridization counterparts. The interactive distances between S(sp^2) atom (*i.e.* S3 and S4) and copper atoms vary between 2.33-2.50 Å while the corresponding figures for S(sp^2) atoms (*i.e.* S1 and S2) are in the range 2.44-2.75 Å. These values the covalent bond distance of Cu-S (2.37 Å).[16] Therefore, in these complexes, the interactions between a Thiram

molecule and Cu$_{20}$ cluster may perform *quasi*-covalent characteristics, conducive to the stability of the bonding, especially formed by complex **A**.

In the next section, the SERS spectrum of the complex **A** in comparison with the normal Raman spectrum of Thiram are projected in order to propose a chemical enhancement mechanism of Thiram adsorbed on the a Cu$_{20}$ cluster.
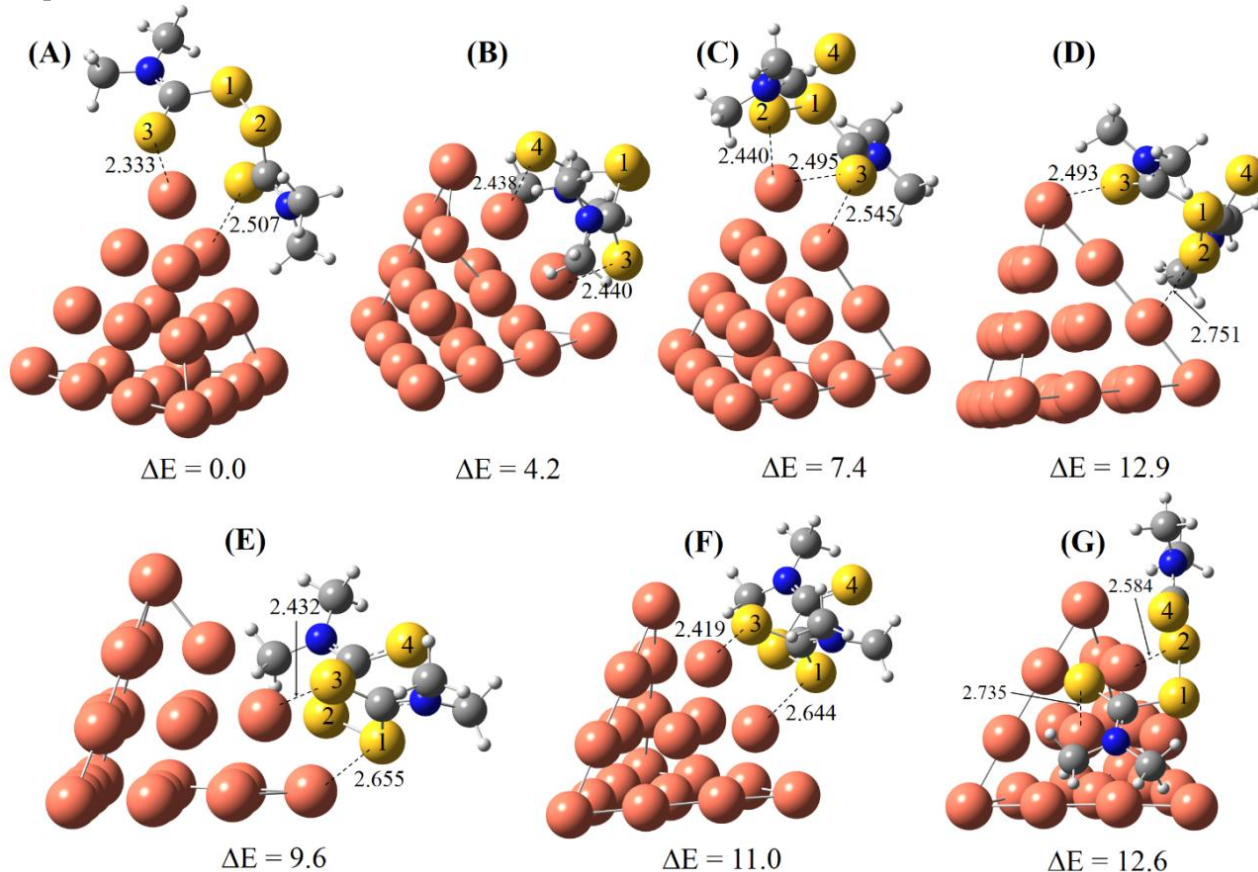
Figure 3: Optimized structures and relative energies (ΔE, in kcal/mol) of seven Thiram-Cu$_{20}$ complexes **A-G**. Unit of distance is Å

3.3. Normal Raman and SERS spectra

Figure 4 compared Raman spectrum of Thiram (figure 4A) and SERS of the most stable Thiram-Cu$_{20}$ (figure 4B), Thiram-Ag$_{20}$ (figure 4C) and Au$_{20}$-Thiram complexes (figure 4D). In addition, the Raman and SERS vibrational assignments are listed in table 1.

In normal Raman spectrum (figure 4A), the highest peak emerges at 1456 cm^{-1} and five other highly pronounced peaks are at 371, 576, 1012, 1414 and 1430 cm^{-1}. They are responsible for the stretching vibrations of C–S, C=S, S–C–S and C–N bonds accompanied with the scissoring bending vibrations of CH$_3$ and CH$_3$NC groups. Regarding the SERS spectra of Thiram-Cu$_{20}$ (figure 4B), Thiram-Ag$_{20}$ (figure 4C) and Thiram-Au$_{20}$ (figure 4D), some

differences with the normal Raman spectrum should be noted. In figure 4B, the most marked peak is found at 982 cm^{-1} and the other significant peaks are also detected at 534, 1398 and 1526 cm^{-1}. They are assigned to the stretching vibrations of S–S, S–C–S, C–N, CH$_3$–N bonds; the scissoring bending vibrations of CH$_3$NCH$_3$, CH$_3$NC groups and the wagging vibrations of CH$_3$, CH$_3$NCH$_3$ groups.

The similar patterns are observed in SERS spectra represented for Thiram-Ag$_{20}$ (figure 4C) and Thiram-Au$_{20}$ (figure 4D). Nevertheless, they experience a slight westward-shift and register a lower overall intensity.

By interacting with the metallic clusters, certain characteristic peaks of Thiram are enhanced. These especially include those at 553 cm^{-1} (which is nearly negligible in normal Raman spectrum of Thiram),

1012 cm^{-1}, 1414 cm^{-1} and 1531 cm^{-1} (table 1). The Raman intensities of these peaks see a respective rise of 122, 102, 50 and 175 times in the SERS spectrum of Thiram-Cu$_{20}$ complex. Otherwise, the indices for Raman enhancement vary from 21 to 104 times for Thiram-Ag$_{20}$ complex and from 12 to 54 times for Thiram-Au$_{20}$ complex. The enhancement is mainly due to the stretching vibrations of CH$_3$N, CN groups and the wagging vibrations of CH$_3$, CH$_3$NCH$_3$ groups. However, some other peaks only witness a marginal-to-non enhanced intensity, such as those at 371, 576, 1430 and 1456 cm^{-1} (figure 4A). In particular, two peaks at 371 and 1430 cm^{-1} are both disappeared in the SERS spectra obtained from all three metal complexes. These peaks relate to the stretching vibration of C–S bond and the scissoring bending vibrations of CH$_3$, CH$_3$NC groups (table 1).

In addition, the Raman intensity of highest peak in SERS spectrum of Thiram-Cu$_{20}$ at 982 cm^{-1} is 2 times higher than that of Thiram-Ag$_{20}$ and 6 times higher than that of Thiram-Au$_{20}$. The other noticeable peaks of Thiram-Cu$_{20}$ complex (*i.e.* 534, 1398 and 1526 cm^{-1}) also have higher Raman activities than the ones of other complexes. Overall, Raman figures obtained for Thiram-Cu$_{20}$ are from

1.2 to 2.4 times higher than those of Thiram-Ag$_{20}$ and from 3.3 to 4.2 times higher than those of Thiram-Au$_{20}$.
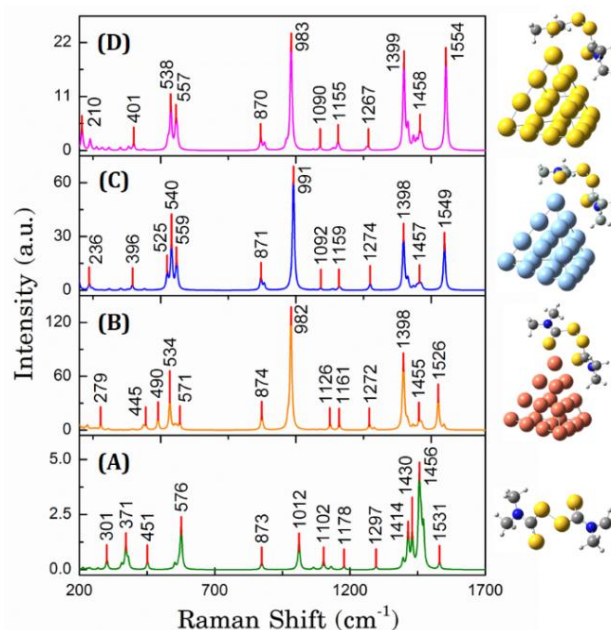
Figure 4: **(A)** Raman spectrum of Thiram and SERS spectra of the most stable complexes: **(B)** Thiram-Cu$_{20}$, **(C)** Thiram-Ag$_{20}$ and **(D)** Thiram-Au$_{20}$

Table 1: Vibrational assignments of normal Raman spectrum of Thiram and SERS spectra of Thiram adsorbed on Cu$_{20}$, Ag$_{20}$ and Au$_{20}$ clusters

Raman	SERS-Cu$_{20}$	SERS-Ag$_{20}$	SERS-Au$_{20}$	Assignments
301 (6.0)	279 (80.2)	236 (47.2)	210 (60.0)	ρ(CH$_3$), σ(NCS), σ(CSS)
371 (14.3)	–	–	–	υ(CS), σ(CH$_3$NC)
451 (2.5)	445 (76.6)	396 (39.9)	401 (20.1)	σ(CS), σ(NCS), σ(CH$_3$NC),
–	490 (171.3)	525 (129.1)	–	ω(SCS), ω(CH$_3$NCH$_3$)
553 (3.6)	534 (439.9)	540 (356.1)	538 (122.3)	υ(SS), ω(SCS), ω(CH$_3$NCH$_3$)
576 (24.9)	571 (109.9)	559 (206.1)	557 (66.3)	σ(CH$_3$NCH$_3$), υ_s(SCS), υ_{as}(CSS)
873 (3.3)	874 (238.8)	871 (105.2)	870 (38.4)	υ_s(CH$_3$NCH$_3$), υ_s(CS)
1012 (18.9)	982 (1924.5)	991 (984.2)	983 (339.7)	υ_{as}(SCS), ω(CH$_3$), υ(CH$_3$N), σ(CH$_3$NC)
1102 (4.3)	1126 (103.9)	1092 (12.4)	1090 (8.3)	ρ(CH$_3$), ω(CH$_3$)
1178 (1.8)	1161 (84.0)	1159 (23.3)	1155 (26.5)	ω(CH$_3$), ρ(CH$_3$), υ_{as}(SC=S)
1297 (1.9)	1272 (112.6)	1274 (58.8)	1267 (12.9)	υ_{as}(CH$_3$NCH$_3$), ω(CH$_3$), υ_{as}(SCS)
1414 (20.7)	1398 (1041.7)	1398 (440.6)	1399 (248)	υ(CN), ω(CH$_3$)
1430 (14.4)	–	–	–	σ(CH$_3$)
1456 (50.4)	1455(157.6)	1457 (53.7)	1458 (46.8)	σ(CH$_3$)
1531 (3.6)	1526 (630.4)	1549 (375.8)	1554 (193.3)	υ(CN), ω(CH$_3$), σ(CH$_3$)

Values in parentheses are calculated Raman activities; (υ) = stretching (with υ_s = symmetric stretching and υ_{as} = anti-symmetric stretching), σ = scissoring bending, ρ = rocking, ω = wagging, τ = twisting.

3.4. Chemical enhancement mechanism

It has been widely accepted that the SERS phenomenon generally stems from electromagnetic and chemical enhancement mechanisms. The former is based on the amplification of the light by the excitation of localized surface plasmonic resonances (LSPRs). The latter primarily refers to charge transfer (CT) process, where the excitation wavelength resonates with the metal−molecule

charge transfer electronic states.[17] The chemical enhancement mechanism of Thiram adsorbed on Au_{20}, Ag_{20} and Cu_{20} clusters is illustrated in figure 5 and table 2.

In particular, figure 5 summarizes total density of states (DOS) spectrum of Thiram, Au_{20}, Ag_{20} and Cu_{20} bare clusters in comparison with the ones of their complexes. The highest occupied molecular orbital (HOMO) and the lowest unoccupied molecular orbital (LUMO) distributions of the studied structures are also displayed with their corresponding energy values (E_H and E_L). The extended values of HOMO-LUMO energy gap (ΔE) are also included. Furthermore, partial density of states (PDOS) analyses provides contributing proportion of Thiram and its coordinated metal clusters in the complexes. LUMO and HOMO are also indicated in order to analyze the CT tendency of electron densities.

Firstly, the difference between HOMO energy and LUMO one, *i.e.* HOMO-LUMO gap or ΔE, is a good indicator to evaluate kinetic stability and chemical stability. Regarding table 2, the ΔE values of the bare clusters accord with the order: $Au_{20} > Ag_{20} > Cu_{20}$ with their corresponding figures 1.89, 1.67 and 1.46 eV, respectively. The narrowest energy gap of Cu_{20} (1.46 eV) indicates its highest reactivity towards Thiram in comparison with Au_{20} and Ag_{20} clusters. Expectedly, the HOMO-LUMO energy gaps of the complexes are also in the similar order: Thiram-Au_{20} (1.41 eV) > Thiram-Ag_{20} (1.28 eV) > Thiram-Cu_{20} (0.95 eV) which shows a reverse order of the stability.

Thus, the narrower energy gaps of the Cu_{20} bare clusters and of the Thiram-Cu_{20} complex are more conducive transfer of electron densities from the ligand to the cluster than those carried out by Ag_{20} and Au_{20} clusters. The easier electronic transfer also explains for the most marked enhancement by SERS for Thiram adsorbed on Cu_{20} (figure 4 and table 1).
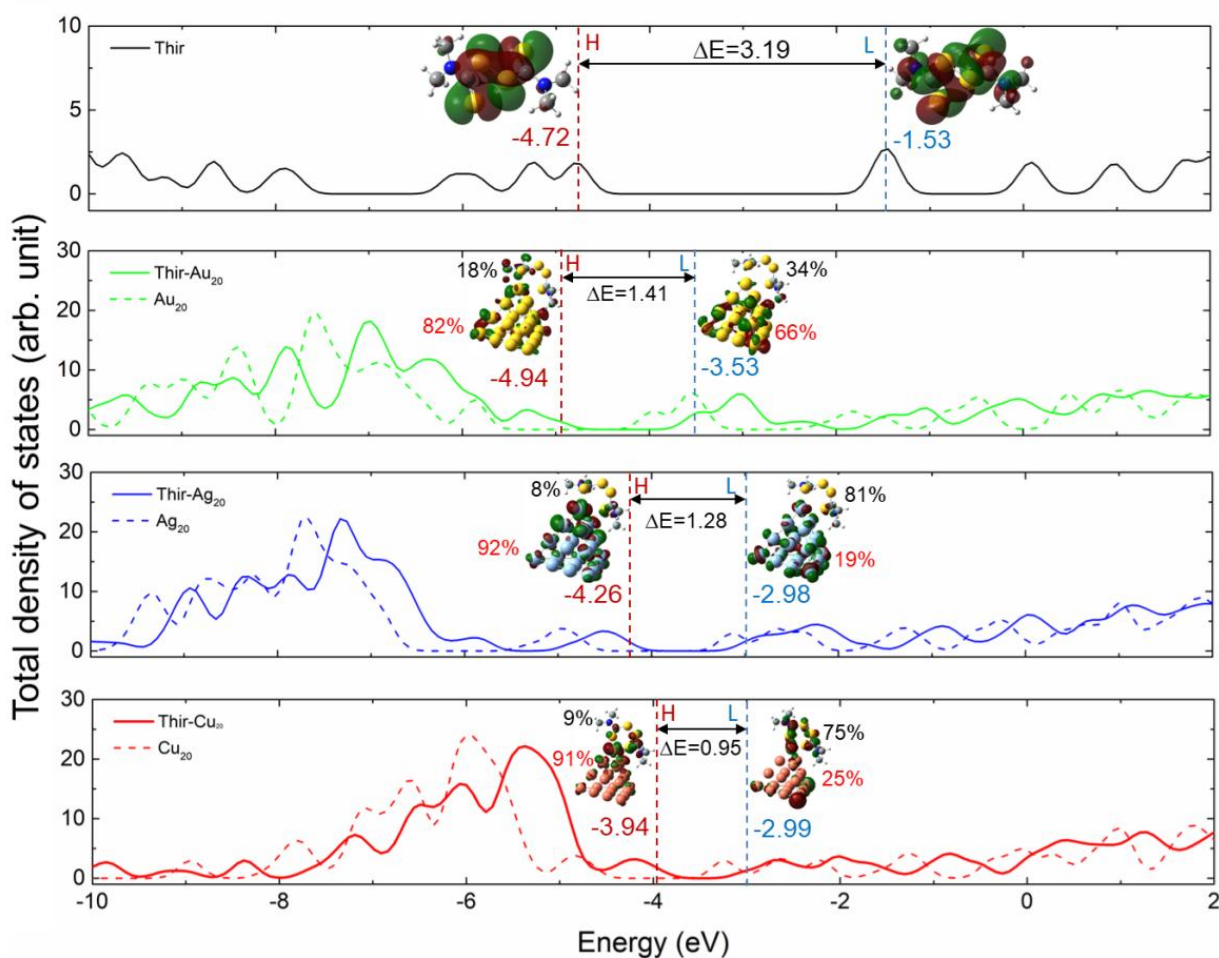
Figure 5: Density of states (DOS) spectrum of Thiram, Au_{20}, Ag_{20} and Cu_{20} bare clusters and their complexes with Thiram (Thir-Au_{20}, Thir-Ag_{20}, Thir-Cu_{20}). LUMO and HOMO distributions are presented on the right and left hand sides of each graphic. The LUMO and HOMO energies are indicated besides the vertical dotted lines with their HOMO-LUMO gap (ΔE) in eV unit. The percentage values correspond to % contribution of Thiram and the metal clusters to LUMO and HOMO orbitals

Secondly, information on the frontier orbitals of the formed complexes clarifies the interaction mechanism between the pesticide molecule and the clusters. And the most important interactions are between HOMO and LUMO of Thiram and those of the clusters. Based on the energy gap, the donation or back-donation of electrons can be revealed. Based on the calculated data in table 2, the energy differences between LUMO of Thiram and HOMO of the clusters are also ranged in declined order: $Au_{20} > Ag_{20} > Cu_{20}$ with the respective values being 4.31, 3.27 and 3.16 eV. In contrast, the energy gaps between LUMO of the Au_{20}, Ag_{20} and Cu_{20} clusters and HOMO of Thiram register are similar order but with considerably smaller values *i.e.* 0.77, 1.59 and 1.49 eV, respectively. These imply that the HOMO-LUMO energy gaps of the forward donation (Thiram→M_{20}, with M represents the metal cluster) are larger than the ones represented for backward donations (M_{20}→Thiram). Hence, Thiram is adsorbed on the metal cluster by donating its electron densities to the cluster. This electron-transfer tendency from organic molecules to metallic cluster is in agreement with the previous studies.[18-20]

Table 2: HOMO and LUMO energies and HOMO-LUMO energy gap

	HOMO	**LUMO**	**ΔE (eV)**
Thir	-4.72	-1.53	3.19
Au_{20}	-5.84	-3.95	1.89
Ag_{20}	-4.80	-3.13	1.67
Cu_{20}	-4.69	-3.23	1.46
Thir-Au_{20}	-4.94	-3.53	1.41
Thir-Ag_{20}	-4.26	-2.98	1.28
Thir-Cu_{20}	-3.94	-2.99	0.95

This observation is further confirmed by analyzing partial density of states (PDOS) (figure 5). The contribution percentages of Thiram and the clusters to LUMO and HOMO indicate that electron densities are always transferred from Thiram to the cluster during the transition from LUMO to HOMO of the complexes. Regarding Thiram-Cu_{20}, 75 % of LUMO electron density is localized on Thiram while only 25 % is found on the Cu_{20} cluster. However, only 9 % of HOMO electron density localizes on Thiram, the corresponding figure for the cluster Cu_{20} is 91 %. This means that 64 % electron densities are transferred from Thiram to the Cu_{20} cluster. Consistent phenomena are observed in regard to Au_{20} and Ag_{20} clusters with the transfer of 16 % and 73 % electron densities, respectively.

4. CONCLUSIONS

Structural, electronic and spectroscopic properties of Thiram and its complexes with Cu_{20}, Ag_{20} and Au_{20} are computationally investigated using DFT method. Normal Raman spectra of Thiram and SERS spectrum of its three complexes are projected. The results show that:

+ Thiram contains two co-planar C_2NCS_2 groups and the interactive sites of Thiram are mainly found at the its sulfur atoms (especially at $S(sp^2)$ atoms, *i.e.* S3 and S4).

+ Thiram interacts with Cu_{20} cluster *via* two or more sulfur atoms. The stability of Thiram-Cu_{20} complexes depends on the number of interaction between Cu_{20} cluster and $S(sp^2)$ atom. The more $S(sp^2)$ atom interact with the Cu_{20} cluster, the more stable the complex is.

+ Normal Raman spectrum of Thiram shows several main peaks including the stretching vibration of C–S bond and scissoring bending vibration of CH_3 groups. Otherwise, the main peaks of SERS spectrum of Thiram-Cu_{20}, Thiram-Ag_{20} and Thiram-Au_{20} complexes relate to N atom and the wagging vibration of CH_3 groups.

+ The SERS chemical enhancement for Thiram derived by Cu_{20} cluster is 2 and 6 times higher than those attained by Ag_{20} and Au_{20} clusters.

+ The most enhanced SERS signals of Thiram adsorbed on Cu_{20} cluster are firstly related to its lowest HOMO-LUMO energy gap by referencing to the Au_{20} and Ag_{20} clusters. Moreover, during the adsorption, the charge transfer prevails through the forward donation direction from Thiram to the metal clusters (Thiram→M_{20}). The energy gap between LUMO of Thiram and HOMO of Cu_{20} is the lowest compared with those of Au_{20} and Ag_{20} cluster. The highest charge transfer from Thiram to cluster is also obtained for the copper one. And this tends to the highest SERS signals obtained when Thiram is adsorbed on the Cu_{20} cluster.

The predicted results suggest a magnification-enhanced and cost-effective copper-based nanomaterial as a potential alternative for expensive inert metals, such as silver or gold, in SERS applications. The most noticeable downside is its sensitivity to ambient oxidization. The disadvantage is less pronounced if the material is expected for portable or one-use purposes.

Conflict of interest. *The authors declare no conflict of interest.*

REFERENCES

1. R. Jayaraj, P. Megha, P. Sreedev. Organochlorine pesticides, their toxic effects on living organisms and their fate in the environment, *Interdiscip. Toxicol.,* **2016**, *9*, 90-100.

2. R. C. Gupta. Carbamate Pesticides, in: Encycl. Toxicol., Elsevier, **2014**, 661-664.

3. V. K. Sharma, J. S. Aulakh, A. K. Malik, Thiram: degradation, applications and analytical methods, *J. Environ. Monit.,* **2003**, *5*, 717-723.

4. B. Gupta, M. Rani, R. Kumar. Degradation of thiram in water, soil and plants: A study by high-performance liquid chromatography, *Biomed. Chromatogr.,* **2012**, *26*, 69-75.

5. H. Dies, M. Siampani, C. Escobedo, A. Docoslis. Direct detection of toxic contaminants in minimally processed food products using dendritic surface-enhanced Raman scattering substrates, *Sensors*, **2018**, *18*, 1-11.

6. P. Stathi, K. C. Christoforidis, A. Tsipis, D. G. Hela, Y. Deligiannakis. Effects of dissolved carboxylates and carbonates on the adsorption properties of thiuram disulfate pesticides, *Environ. Sci. Technol.,* **2006**, *40*, 221-227.

7. G. M. Linz, M. L. Avery, R. A. Dolbeer, eds. Ecology and Management of Blackbirds (Icteridae)

8. J. S. Kang, S. Y. Hwang, C. J. Lee, M. S. Lee. SERS of dithiocarbamate pesticides adsorbed on silver surface; Thiram, *Bull. Korean Chem. Soc.*, **2002**, *23*, 1604-1610.

9. A. K. Verma, R. K. Soni. Silver nanodendrites for ultralow detection of thiram based on surface-enhanced Raman spectroscopy, *Nanotechnology*, **2019**, *30,* 385502-385516.

10. K. Rajalakshmi, M. Vetrivel. Optimization and vibrational study of 2-propylpyridine-4-carbothioamide by DFT - A theoretical study, *Int. J. ChemTech Res*., **2016**, *9*, 306-316.

11. N. T. T. An, D. Q. Dao, P. C. Nam, B. T. Huy, H. N. Tran. Surface enhanced Raman scattering of melamine on silver substrate: An experimental and DFT study*, Spectrochim. Acta Part A Mol. Biomol. Spectrosc.,* **2016**, *169*, 230-237.

12. M. J. Frisch, G. W. Trucks, H. B. Schlegel, G. E. Scuseria, M. A. Robb et al., Gaussian 16 Rev. A.03, **2016**.

13. J. P. Perdew, K. Burke, M. Ernzerhof. Errata: Generalized gradient approximation made simple, *Phys. Rev. Lett.,* **1997**, *78*, 1396.

14. M. K. Kesharwani, B. Brauer, J. M. L. Martin. Frequency and zero-point vibrational energy scale factors for double-hybrid density functionals (and other selected methods): Can anharmonic force fields be avoided?, *J. Phys. Chem. A*., **2015**, *119*, 1701-1714.

in North America, CRC Press, Boca Raton: CRC Press, **2017**.

Corresponding author: **Dao Duy Quang**
Institute of Research and Development, Duy Tan University
3, Quang Trung, Da Nang, 50000, Viet Nam
E-mail: daoduyquang@duytan.edu.vn.